Chinese Chemical Letters 37 (2026) 111790

Contents lists available at ScienceDirect

Chinese Chemical Letters

journal homepage: www.elsevier.com/locate/cclet

Bis-trimethylammonium pillar[5]arene and biphenyldisulfonic acid-based ionic pair assembled single crystals for iodine adsorption

Ting Zhang[a,b], Jia Chen[b], Mingxia Sun[b], Juanjuan Wang[b], Lulu Wang[a,*], Shuzhe Guan[a,*], Hongdeng Qiu[b,c,*]

[a] State Key Laboratory of Chemistry and Utilization of Carbon Based Energy Resources, College of Chemistry, Xinjiang University, Urumqi 830017, China
[b] CAS Key Laboratory of Chemistry of Northwestern Plant Resources and Key Laboratory for Natural Medicine of Gansu Province, Lanzhou Institute of Chemical Physics, Chinese Academy of Sciences, Lanzhou 730000, China
[c] Key Laboratory of Rare Earths, Ganjiang Innovation Academy, Chinese Academy of Sciences, Ganzhou 341000, China

ARTICLE INFO

Article history:
Received 5 March 2025
Revised 5 July 2025
Accepted 4 September 2025
Available online 7 September 2025

Keywords:
Ionic self-assembly
Pillar[5]arene
Ionic single crystals
Iodine adsorption
Supramolecular chemistry

ABSTRACT

In this work, bis-trimethylammonium pillar[5]arene (TP5) was synthesized for ionic pair assembly with 4,4′-biphenyldisulfonic acid (BA) to prepare a new kind of ionic single crystals (TP5-BA). The single crystal structure revealed that TP5-BA adopted an ordered cross-stacked arrangement under the combined influence of electrostatic interactions and π-π stacking forces. It is worth noting that TP5-BA exhibited exceptional performance in the adsorption of iodine vapor, with an adsorption capacity as high as 3.27 g/g. After 6 days, its retention rate remained at a high level of 99.71 %. This finding may open up a new direction in supramolecular chemistry with ionic pair self-assembly, not only for the development of novel iodine adsorbent materials but also for many other potential applications such as catalysis and energy.

© 2026 Published by Elsevier B.V. on behalf of Chinese Chemical Society and Institute of Materia Medica, Chinese Academy of Medical Sciences.

Since Ogoshi *et al.* first discovered pillar[5]arene in 2008 [1], this compound has garnered widespread attention in the field of supramolecular chemistry due to its unique electron-rich cavity [2], symmetric rigid structure [3], pronounced planar chirality [4], ease of functionalization [5,6], and exceptional host-guest recognition capabilities [7]. These features enable pillar[5]arenes to form diverse supramolecular architectures through self-assembly, including host-guest self-assembly achieved *via* non-covalent interactions with ions, drug molecules, and other guests [8–11]. Pillararenes could bind with other molecules through mechanical interlocking, thereby constructing complex supramolecular structures, such as rotaxanes [12,13]. Pillararenes can also serve as ligands to self-assemble with metal ions, resulting in the formation of stable metal-coordinated complexes [14]. Pillararenes were capable of self-assembling into various structures, such as nanocapsules and vesicles, and these nanoscale entities demonstrated significant potential for applications in materials science and nanotechnology [15,16].

The self-assembly strategies of pillararenes exhibited broad application prospects in materials science, drug delivery systems, sensor engineering, biomedical applications, and nanotechnology [14,17–20]. It is noteworthy that pillararenes demonstrated significant advantages in the capture of radioactive iodine. Materials based on pillararenes for iodine adsorption have already been developed [21–24]. However, despite these advancements, the exploration of pillar[5]arene-based ionic self-assembly materials driven by electrostatic interactions remains unexplored, representing a significant gap in the field.

In this work, bis-trimethylammonium pillar[5]arene (TP5) was successfully synthesized as cationic blocks, and 4,4′-biphenyldisulfonic acid (BA) was used as anionic blocks, two oppositive ionic blocks can be self-assembled by electrostatic interactions, which led to the preparation of a novel pillar[5]arene-based ionic single crystals (TP5-BA). Additionally, benzene rings, trimethylammonium, and sulfonic acid groups in the TP5-BA molecule played a crucial role in efficient iodine adsorption. The development of TP5-BA not only opened up a new field in supramolecular chemistry and self-assembly strategy, but also significantly advanced the progress of this kind of innovative materials for other fields.

Hydroquinone and 1,4-dibromobutane underwent a nucleophilic substitution reaction to synthesize 1,4-bis(4-bromobutoxy)-benzene (BB). Subsequently, under suitable reaction conditions, BB reacted with 1,4-dimethoxybenzene through a copolymer-

* Corresponding authors.
E-mail addresses: 006785@xju.edu.cn.com (L. Wang), 254425698@qq.com (S. Guan), hdqiu@licp.cas.cn (H. Qiu).

https://doi.org/10.1016/j.cclet.2025.111790
1001-8417/© 2026 Published by Elsevier B.V. on behalf of Chinese Chemical Society and Institute of Materia Medica, Chinese Academy of Medical Sciences.

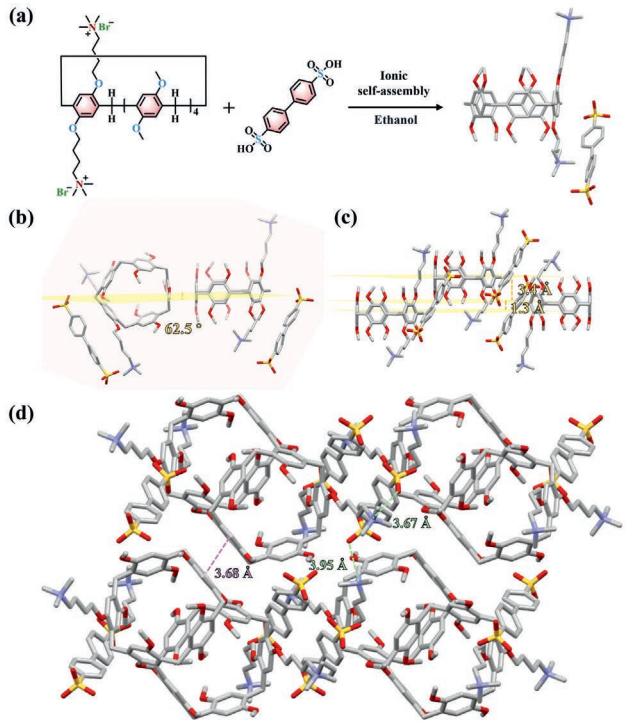


Fig. 1. (a) Synthesis and crystal structure of TP5-BA. (b) Dihedral angles of TP5 in TP5-BA. (c) The distance between TP5 planes in TP5-BA. (d) The packing mode of TP5-BA is viewed down the crystallographic b-axis.

ization reaction to produce 1,4-bis(bromobutoxy)copillar[5]arene (BBP5). Following this, BBP5 reacted with trimethylamine through a nucleophilic substitution reaction, successfully preparing bis-trimethylammonium pillar[5]arene (TP5) [25,26]. The detailed synthesis process and structural characteristics of TP5 can be found in Scheme S1 and Figs. S1-S6 (Supporting information). These synthetic steps effectively introduced the target functional groups, laying the foundation for the functionalization of pillararenes.

Then, TP5 was employed as the cationic blocks, and 4,4′-biphenyldisulfonic acid (BA) was selected as the anionic blocks. The TP5 molecule contained two positively charged tertiary amine groups, facilitating effective ionic self-assembly with the BA anion. Utilizing the ionic pair self-assembly strategy, a self-assembled ionic single crystal based on pillar[5]arene was successfully constructed. At room temperature, the TP5-BA ionic single crystal, suitable for X-ray diffraction analysis, was successfully prepared by the slow evaporation of an absolute ethanol solution (CCDC No. 2415288).

Fourier transform infrared spectroscopy (FT-IR) analysis successfully identified the specific functional groups in the prepared TP5-BA material. Two new distinct characteristic peaks observed at 613.2 and 822.3 cm^{-1} confirmed their correspondence to the symmetric -SO_3 bending vibrations (Fig. S7 in Supporting information) [27]. This finding further substantiated the successful self-assembly between BA and TP5.

The synthesis of TP5-BA was illustrated in Fig. 1a. The BA molecule was located outside the cavity formed by the TP5; a one-to-one correspondence was established between the TP5 and BA units. Each TP5 layer had a dihedral angle of approximately 62.5° concerning the adjacent TP5 layer (Fig. 1b). Additionally, TP5 molecules self-assembled through a layered, alternating stacking arrangement, resulting in a regular lattice structure. Within this structure, TP5 molecules maintained a parallel arrangement, with one set of TP5 layers exhibiting alternating interlayer distances of 3.4 Å and 1.3 Å; another set of TP5 layers alternated interlayer distances between 4.8 Å and 11.2 Å (Fig. 1c and Fig. S8 in Supporting information). This variation in interlayer spacing represented the diversity of interlayer spaces within the lattice. In the TP5-BA crystal structure, BA molecules were intercalated between adjacent TP5 molecules. The alkyl chains of the TP5 molecules underwent significant conformational adjustments to facilitate electrostatic interactions with the oppositely charged BA molecules. π-π stacking interactions were identified between the adjacent and staggered TP5 molecular layers, with a center-to-center distance of 3.68 Å. The distance between the cation and anion is 3.95 Å and 3.67 Å, as shown in Fig. 1d. The synergistic effects of these π-π stacking and electrostatic interactions were instrumental in stabilizing the self-assembled supramolecular ionic structure.

The thermal stability of TP5-BA was investigated by thermogravimetric analysis (TGA) (Fig. 2a). TGA results showed that the material exhibited a weight loss of approximately 7 % in the temperature range of 0–330 °C, which was primarily attributed to the evaporation of residual solvents. When the temperature was increased to 330–589 °C, significant mass loss occurred due to thermal decomposition of the organic components. Notably, the onset decomposition temperature of TP5-BA reached 330 °C, demonstrating its excellent thermal stability. The Brunauer-Emmett-Teller (BET) surface areas were determined. The permanent porosity was determined from the CO_2 adsorption-desorption isotherms at 195 K, with the calculated surface area of micropores being 63.91 m^2/g. The pore size distribution analysis of TP5-BA material revealed that its pores were predominantly distributed within the range of 0.50 - 1.03 nm, indicating the presence of microporous characteristics (Fig. 2b). Conventional N_2 adsorption failed to provide a reasonable surface area value due to the low affinity of nonpolar nitrogen molecules for highly polar surfaces (Fig. 2c) [28–30]. The scanning electron microscopy (SEM) and energy-dispersive X-ray spectroscopy (EDS) mapping analyses, as depicted in Figs. 2d and e, elucidated the surface morphology and elemental distribution within TP5-BA. TP5-BA exhibited a relatively smooth surface morphology, and the uniform distribution of C, N, O, and S elements confirmed the excellent growth of TP5-BA.

TP5-BA contained electron-rich moieties, which could act as electron donors to facilitate interactions with iodine molecules [31,32]. The adsorption capacity of TP5-BA for iodine vapor was evaluated. After the adsorption process, the surface topography of the material was observed to have roughened, with the emergence of multiple irregular protrusions (Fig. 3a). Subsequent EDS mapping analysis revealed that iodine had been uniformly distributed across the surface of the adsorbent TP5-BA following iodine adsorption (Fig. 3b), signifying the successful capture of iodine vapor by the adsorbent TP5-BA. The maximum adsorption capacities were determined by weighing the mass of adsorbents before and after adsorption. As shown in Fig. 3c, TP5-BA exhibited relatively fast adsorption rates in the initial 30 h, with almost a linear increase trend. After approximately 70 h, the adsorption reached equilibrium, and the adsorption capacity was 3.27 g/g (Eq. S1 in Supporting information).

Considering the effective adsorption of iodine vapor by TP5-BA, the kinetic adsorption processes were investigated for a deeper insight into its adsorption behavior. The *pseudo*-first-order model assumed that the internal diffusion process is the rate-controlling step, while the *pseudo*-second-order kinetic model suggested that the chemical adsorption of adsorbate molecules on active sites is the rate-controlling step [33]. The results indicated that the iodine adsorption process by TP5-BA exhibited high linearity with both the *pseudo*-first-order kinetic model and the *pseudo*-second-order kinetic model, with linear correlation coefficients (R^2) of 0.980 and 0.990, respectively, both close to 1 (Eqs. S2 and S3 in Supporting information). The kinetic study suggested that the adsorption process involved both physical and chemical adsorption, but was pre-

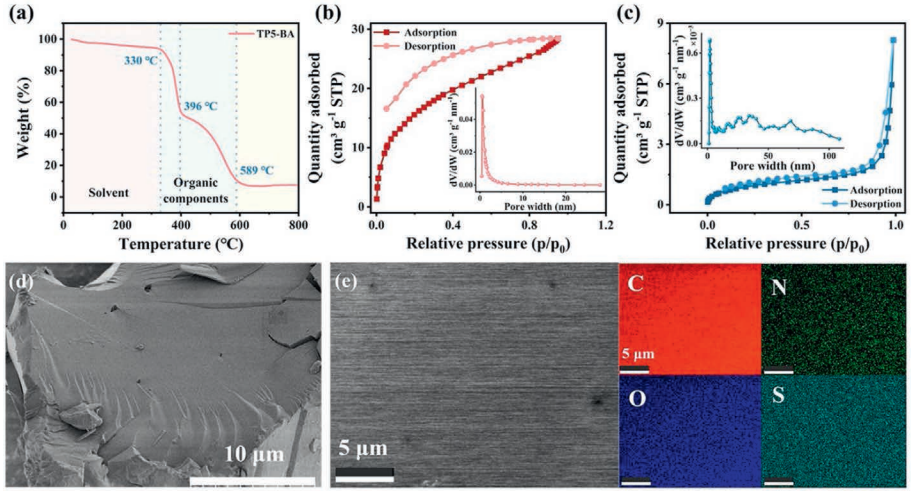


Fig. 2. Characterizations of TP5-BA. (a) TGA curves, (b) CO_2 and (c) N_2 adsorption-desorption isotherms for TP5-BA. Inset: pore size distribution profile of TP5-BA. (d) SEM images, and (e) elemental mapping of TP5-BA.

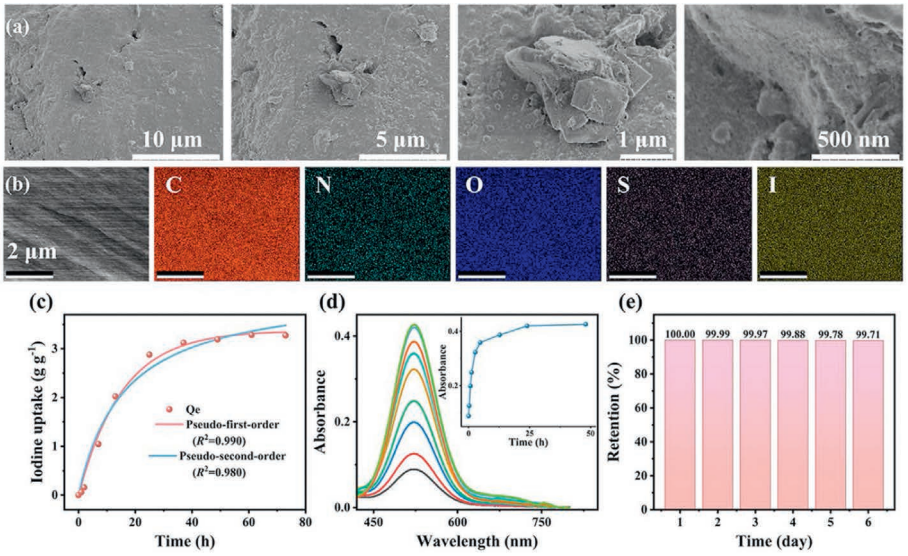


Fig. 3. (a) SEM images of TP5-BA@I_2. (b) Elemental mapping of TP5-BA after adsorption of iodine. (c) Time-dependent iodine adsorption by TP5-BA at 343.15 K and analysis of kinetic models for iodine adsorption onto TP5-BA. (d) Time-dependent UV/vis absorption spectra of cyclohexane upon addition of TP5-BA@I_2. Inset: I_2 absorbance at 522 nm at various times. (e) Iodine retention of TP5-BA@I_2.

dominantly dominated by physical adsorption [34]. Additionally, the following experiments and characterization results confirmed this viewpoint.

Upon dissolving the TP5-BA@I_2 in cyclohexane, it was noted that iodine was released swiftly. Utilizing a pre-established standard curve, the absorbance at 522 nm was employed to quantify the iodine concentration within the solution (Fig. S9 in Supporting information). The data revealed that a mere 60 % of the iodine was liberated, suggesting that the residual iodine remained firmly adsorbed to TP5-BA *via* chemical interactions (Fig. 3d).

Furthermore, a comparison of the thermogravimetric analysis (TGA) of TP5-BA with its iodine-adsorbed counterpart, TP5-BA@I_2, demonstrated a clear distinction (Fig. S10 in Supporting information). At 300 °C, the release rate of TP5-BA@I_2 reached 61.61 %, which was significantly lower than the decomposition temperature of the pristine TP5-BA sample. This observation suggested a physisorption process characterized by weak interactions between the I_2 molecules and the TP5-BA, comparable to the adsorption of iodine in the vapor phase by the gravimetric method mentioned above [35]. The residual weight percentage of TP5-BA@I_2 at 800 °C was significantly higher than that of TP5-BA before adsorption, which could be attributed to the relatively strong binding force between iodine and TP5-BA. The incorporation of iodine has improved the thermal stability of the material [36].

The weight of iodine loaded onto TP5-BA still retained a high rate of 99.71 % after being exposed to ambient air for 6 days (Fig. 3e) (Eq. S4 in Supporting information). This indicated a robust interaction between iodine and TP5-BA, suggesting that iodine did not leach out of the pores of TP5-BA [37,38]. After three adsorption-desorption cycles, TP5-BA maintained a relative iodine vapor adsorption capacity of 48.81 % (Fig. S11 and Eq. S5 in Supporting information), demonstrating good cycling stability.

Upon comparing the FT-IR spectra of TP5-BA and TP5-BA@I_2, a marked decrease in the intensity of the infrared absorption peaks was observed for TP5-BA@I_2 (Fig. 4a). This phenomenon was likely due to the iodine molecules covering the material surface, as well as the interaction between the iodine molecules and the functional groups on the material surface, which consequently led to the reduction in the intensity of the infrared absorption peaks [39].

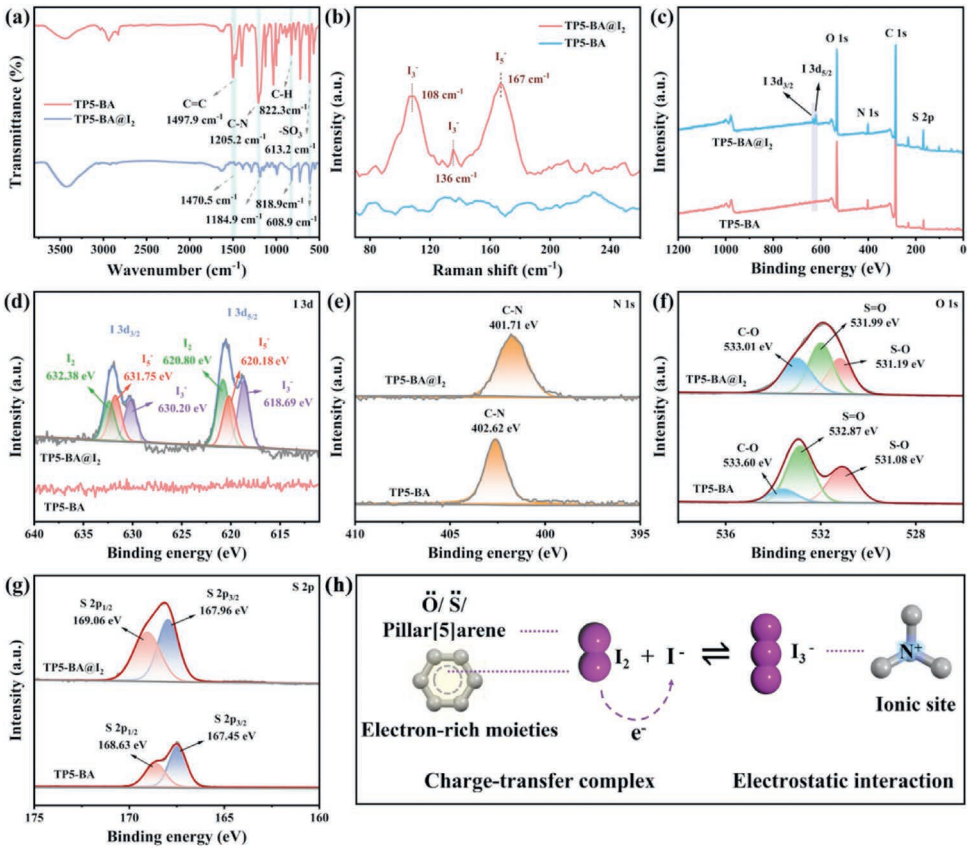


Fig. 4. Study on the mechanism of TP5-BA before and after iodine adsorption. (a) FT-IR spectra. (b) Raman spectra. (c) Full survey XPS spectrum. XPS spectra: (d) I 3d, (e) N 1s, (f) O 1s, and (g) S 2p. (h) Schematic diagram of a possible adsorption process.

The FT-IR spectroscopic analysis revealed that in TP5-BA, the absorption peaks for the C=C and C–H bonds in the phenyl ring were located at 1497.9 cm^{-1} and 822.3 cm^{-1}, respectively; the C–N bond absorption peak was at 1205.2 cm^{-1}; and the -SO_3 group absorption peak appeared at 613.2 cm^{-1} [40–42]. Following the adsorption of iodine by TP5, a blue shift of these functional group absorption peaks was observed; the C=C and C–H bond absorption peaks in the phenyl ring shifted to 1470.5 cm^{-1} and 818.9 cm^{-1}, respectively; the C–N bond absorption peak shifted to 1184.9 cm^{-1}; and the -SO_3 group absorption peak moved to 608.9 cm^{-1}. The variations in the infrared spectrum indicated that during the iodine adsorption process on TP5-BA, the phenyl ring, trimethylammonium, and sulfonic acid functional groups likely played a crucial role. The changes in the vibrational modes of these functional groups resulted in the blue shift and a reduction in the intensity of the absorption peaks. To further explore the iodine species present during the iodine adsorption onto TP5, Raman spectroscopy analyses were conducted on TP5-BA and TP5-BA@I_2. In the Raman spectrum of TP5-BA@I_2, the bands at 108 cm^{-1} and 136 cm^{-1} corresponded to the symmetric and asymmetric stretching vibrations of I_3^-, respectively, and the band at 167 cm^{-1} corresponded to the stretching vibration of I_5^- (Fig. 4b) [31,43]. These data indicated that iodine existed in the form of polyiodide species during the adsorption process.

Additionally, the X-ray photoelectron spectra (XPS) analysis revealed the electron-rich sites within the TP5-BA material to possess the capability of capturing iodine. As shown in Fig. 4c, the analysis of the full XPS spectrum conducted after iodine capture revealed the presence of two characteristic peaks corresponding to I 3d, indicating that TP5-BA had effectively captured iodine vapor. In the case of the I 3d fine XPS spectra, the peaks at binding energies of 632.38 eV and 620.80 eV corresponded to the characteristic peaks of I_2. Meanwhile, the peaks at binding energies of 631.75 eV and 620.18 eV were attributed to I_3^-, and the peaks at 630.20 eV and 618.69 eV were associated with I_5^- (Fig. 4d). The I 3d fine spectrum data indicated that during the iodine adsorption process on TP5-BA, an electron transfer occurred between iodine molecules and TP5-BA, resulting in the formation of polyiodide anions [44–46].

A shift in the N 1s XPS spectral signal was observed after the adsorption of iodine by TP5-BA (Fig. 4e). The binding energy of the N 1s electrons, corresponding to the C–N bond in trimethylammonium, shifted from 402.62 eV to 401.71 eV after the capture of iodide [47]. The interaction between the trimethylammonium sites and iodide was further confirmed by the N 1s fine XPS spectra [42,48]. Significant shifts in the binding energy peaks within the O 1s and S 2p spectral regions were identified during XPS analysis. In the O 1s spectrum of TP5-BA, three distinct peaks were observed: at 531.08 eV, attributed to the S-O functional group; at 532.87 eV, attributed to the S=O functional group; and at 533.60 eV, attributed to the C–O functional group. After iodine adsorption, the corresponding peaks in the O 1s spectrum of TP5-BA@I_2 shifted as follows: The S-O peak to 531.19 eV, the S=O peak to 531.99 eV, and the C–O peak to 533.01 eV (Fig. 4f) [49]. In the S 2p spectrum, shifts in binding energy were also observed. After the adsorption of iodine on TP5-BA, the binding energy of the S $2p_{3/2}$ peak shifted from 167.45 eV to 167.96 eV, and that of the S $2p_{1/2}$ peak shifted from 168.63 eV to 169.06 eV (Fig. 4g) [50]. These shifts in the binding energies of both O and S indicated that the interaction between the sulfonic acid functional groups and iodine was a significant aspect of the adsorption process. XPS analysis confirmed the presence of I_2, I_3^-, and I_5^- species upon iodine adsorp-

tion, with concurrent shifts in the binding energies of N, O, and S, indicating chemical interactions between iodine and the surface functional groups. The comprehensive characterizations by FT-IR, Raman, and XPS revealed that the electron-rich groups in TP5-BA, including the benzene ring, trimethylammonium, and sulfonic acid groups, played a crucial role in the adsorption process of iodine.

Based on studies of sorption performance and mechanism, it was proposed that the TP5-BA ion crystal material possesses numerous adsorption sites and a suitable pore size, facilitating the adsorption and retention of iodine vapor. In TP5-BA, electron-rich features such as S and O heteroatoms, abundant aromatic rings, and an electron-rich cavity in the pillar[5]arene were present. The Lewis acid-base interaction between the electron-rich active site and iodine facilitated the charge transfer from the lone pair of electrons to the antibonding orbitals (σ^*) of iodine, forming charge-transfer complexes [51]. During this process, I_2 was polarized to I^-, as it accepted an electron in the reaction, represented as I^-. The charge-transfer complexes adsorbed additional iodine molecules to generate polyiodide anions further. Furthermore, strong coulombic electrostatic interactions between the abundant trimethylammonium sites in the TP5-BA and polyiodide anions were formed (Fig. 4h) [42,45,52–54].

In summary, we successfully designed and synthesized a novel pillar[5]arene ionic self-assembled single crystal, which was driven by electrostatic interactions following the introduction of 4,4′-biphenyldisulfonic acid to form ionic pairs with bis-trimethylammonium pillar[5]arene. X-ray single-crystal analysis indicated that TP5-BA adopted a cross-stacking arrangement. The comprehensive research results showed that the maximum adsorption capacity of TP5-BA for iodine vapor reached 3.27 g/g. The adsorption process involved a mixed mechanism of physical and chemical adsorption, in which the benzene rings, trimethylammonium, and sulfonic acid groups within TP5-BA played crucial roles, and TP5-BA exhibited excellent adsorption performance. The appropriate pore size of TP5-BA ensured the efficient entry of iodine molecules into its structure. Moreover, the charge-transfer complexes formed between the electron-rich groups of TP5-BA and iodine molecules adsorbed additional iodine molecules, thereby facilitating the formation of polyiodide anions. At last, we can speculate that this kind of pillar[5]arene-based ionic crystals may have many other potential applications.

Declaration of competing interest

The authors declare that they have no known competing financial interests or personal relationships that could have appeared to influence the work reported in this paper.

CRediT authorship contribution statement

Ting Zhang: Writing – original draft, Methodology, Investigation, Formal analysis, Conceptualization. **Jia Chen:** Software, Project administration, Investigation, Formal analysis. **Mingxia Sun:** Investigation, Formal analysis. **Juanjuan Wang:** Methodology, Investigation. **Lulu Wang:** Writing – original draft, Supervision, Investigation. **Shuzhe Guan:** Writing – original draft, Supervision, Methodology, Conceptualization. **Hongdeng Qiu:** Writing – review & editing, Visualization, Formal analysis, Conceptualization.

Acknowledgments

This work was supported by the National Natural Science Foundation of China (Nos. 22374159 and 22474141), the Gansu Province Outstanding Youth Fund project (No. 24JRRA042), and the Youth Innovation Promotion Association CAS (No. 2021420).

Supplementary materials

Supplementary material associated with this article can be found, in the online version, at doi:10.1016/j.cclet.2025.111790.

References

[1] T. Ogoshi, S. Kanai, S. Fujinami, et al., J. Am. Chem. Soc. 130 (2008) 5022–5023.
[2] S. Bleus, W. Dehaen, Coord. Chem. Rev. 509 (2024) 215762.
[3] H. Li, X. Wang, C. Shi, et al., Chin. Chem. Lett. 34 (2023) 107606.
[4] K. Kato, S. Fa, T. Ogoshi, Angew. Chem. Int. Ed. 62 (2023) e202308316.
[5] X.N. Han, Y. Han, C.F. Chen, Chem. Soc. Rev. 52 (2023) 3265–3298.
[6] H. Li, Y. Qi, J. Chen, et al., Chin. Chem. Lett. 35 (2024) 109659.
[7] Y. Hou, C. Mu, Y. Shi, et al., Aggregate 5 (2024) e628.
[8] M. Li, Y. Liu, L. Shao, et al., J. Am. Chem. Soc. 145 (2022) 667–675.
[9] B. Hua, L. Shao, Z. Zhang, et al., J. Am. Chem. Soc. 141 (2019) 15008–15012.
[10] B. Lu, J. Xia, Y. Huang, et al., Chem. Commun. 59 (2023) 12091–12099.
[11] K. Zhang, X.-Y. Lou, Y. Wang, et al., Chin. Chem. Lett. 36 (2025) 110464.
[12] X. Chi, X. Ji, D. Xia, et al., J. Am. Chem. Soc. 137 (2015) 1440–1443.
[13] X. Chi, G. Yu, L. Shao, et al., J. Am. Chem. Soc. 138 (2016) 3168–3174.
[14] Y. Fang, Y. Deng, W. Dehaen, Coord. Chem. Rev. 415 (2020) 213313.
[15] B. Lu, Z. Zhang, Y. Ji, et al., Sci. China Chem. 65 (2022) 1134–1141.
[16] C. Shi, H. Li, X. Shi, et al., Chin. Chem. Lett. 33 (2022) 3613–3622.
[17] H. Zhang, Z. Liu, F. Xin, et al., Coord. Chem. Rev. 420 (2020) 213425.
[18] X. Li, M. Shen, J. Yang, et al., Adv. Mater. 36 (2024) 2313317.
[19] S. Cao, L. Zhou, C. Liu, et al., Biosens. Bioelectron. 181 (2021) 113164.
[20] X.Y. Lou, K. Zhang, Y. Bai, et al., Angew. Chem. Int. Ed. 64 (2025) e202414611.
[21] K. Jie, Y. Zhou, Q. Sun, et al., Nat. Commun. 11 (2020) 1086.
[22] K. Jie, Y. Zhou, E. Li, et al., J. Am. Chem. Soc. 139 (2017) 15320–15323.
[23] Y. Chen, X. Song, A. Li, et al., Adv. Mater. 36 (2024) 2402885.
[24] Z.N. Chen, L.P. Zhang, H.L. Wu, et al., Chem. Sci. 15 (2024) 13191–13200.
[25] Y.M. Zhang, Y.F. Li, H. Fang, et al., Soft Matter 14 (2018) 8529–8536.
[26] M. Zeng, J. Tan, K. Chen, et al., ACS Appl. Mater. Interfaces 11 (2019) 8537–8544.
[27] L. Pejov, M. Ristova, B. Soptrajanov, J. Mol. Struct. 555 (2000) 341–349.
[28] S. Zhang, J. Fu, S. Das, et al., Angew. Chem. Int. Ed. 61 (2022) e202212962.
[29] X. Suo, X. Cui, L. Yang, et al., Adv. Mater. 32 (2020) 1907601.
[30] S. Yu, G.L. Xing, L.H. Chen, et al., Adv. Mater. 32 (2020) 2003270.
[31] Q. Mao, S. Yang, J. Zhang, et al., Adv. Sci. 11 (2024) 2408494.
[32] X. Liu, A. Zhang, R. Ma, et al., Chin. Chem. Lett. 33 (2022) 3549–3555.
[33] R. Yu, Y. Shi, D. Yang, et al., ACS Appl. Mater. Interfaces 9 (2017) 21809–21819.
[34] W.H. Lee, J.O. Kim, Chem. Eng. J. 453 (2023) 139817.
[35] M.M. Khan, K.W. Chen, Y.T. Chen, et al., Sep. Purif. Technol. 354 (2025) 128746.
[36] S.N. Liu, H.N. Wang, M.L. Feng, et al., ACS Appl. Nano Mater. 6 (2022) 656–663.
[37] Y. Ran, M. Yang, J. Li, et al., Sep. Purif. Technol. 355 (2025) 129603.
[38] J. Chang, H. Li, J. Zhao, et al., Chem. Sci. 12 (2021) 8452–8457.
[39] S. Fajal, W. Mandal, A. Torris, et al., Nat. Commun. 15 (2024) 1278.
[40] N. Farooq, M.A. Malik, A.A. Hashmi, Chem. Eng. J. 498 (2024) 154894.
[41] K. Cheng, H. Li, J.R. Wang, et al., Small 19 (2023) 2301998.
[42] X. Wang, X. Guo, J. Qi, et al., Sep. Purif. Technol. 355 (2025) 129646.
[43] B. Jiang, Y. Qi, X. Li, et al., Chin. Chem. Lett. 33 (2022) 3556–3560.
[44] P. Su, S. Chen, Z. Yang, et al., Chin. Chem. Lett. 35 (2024) 109357.
[45] Y.X. Zheng, X. Wu, W.G. Yang, et al., J. Hazard. Mater. 480 (2024) 135713.
[46] L. Zhang, Y.T. Luo, J.Q. Fan, et al., J. Hazard. Mater. 465 (2024) 133488.
[47] L.P. Ramírez, N. Fornefeld, F. Bournel, et al., J. Phys. Chem. C 126 (2022) 2548–2560.
[48] J. Yang, W. Tai, F. Wu, et al., Chemosphere 292 (2022) 133401.
[49] J.Y. Liu, L. Zhang, J. Fu, et al., Sep. Purif. Technol. 331 (2024) 125664.
[50] Y. Peng, Z.J. Guan, K.K. Liu, et al., CCS Chem. 7 (2025) 1997–2015.
[51] S. Pourebrahimi, M. Pirooz, A. De Visscher, et al., J. Environ. Chem. Eng. 10 (2022) 107805.
[52] D.K.L. Harijan, V. Chandra, T. Yoon, et al., J. Hazard. Mater. 344 (2018) 576–584.
[53] M.A.S. Andrade Jr., A.F. Nogueira, K. Miettunen, et al., J. Power Sources 325 (2016) 161–170.
[54] D. Li, G. Wu, Y.K. Zhu, et al., Angew. Chem. Int. Ed. 136 (2024) e202411261.